

EFFECTS OF BOLT SPACING, BOLT LENGTH, AND ROOF SPAN ON BOLT LOADING IN A TRONA MINE

S. P. Signer and R. Raines

Spokane Research Laboratory, National Institute for Occupational Safety and Health, Spokane, WA, USA

Abstract

Researchers from the Spokane Research Laboratory of the National Institute for Occupational Safety and Health installed 39 instrumented, fully grouted bolts at six test sites in a trona mine retreat panel to study mine roof stability for the improvement of workplace safety. Variables at each test site included bolt spacing, bolt length, roof span, and location in the panel layout. At most test sites, two rows of instrumented bolts were installed, one in or near the intersection created during development and the other in or near the intersection created during second-pass mining.

The most significant factor affecting bolt load was roofspan. The highest loads were on the bolts installed in the intersections of the 6-m-wide entry. Mining-induced stress resulting from panel layout was the next most significant factor affecting bolt loading. Minor variations in bolt loading could be attributed to changes in bolt spacing and bolt length. Gas pressure release in the immediate roof contributed to some bolts showing compressional loading during gas bleed-off.

INTRODUCTION

Strain gauges were first used by researchers in the mid-1970's to measure loading on fully grouted roof bolts (Dunham 1974; Farmer 1975; Sawyer and Karabin 1975) and have been proven to be quite successful under both laboratory (Serbousek and Signer 1985, 1987; McHugh and Signer 1999) and underground (Gale 1987) conditions. The Bureau of Mines conducted a study on grouted bolt loading in 1988 (Signer and Jones 1990) and found that loads on grouted bolts were much higher than loads predicted by suspension theory. Follow-up tests confirmed the initial findings (Maleki et al. 1994; Larson et

al. 1995; Signer et al. 1993; Signer and Lewis 1998). The Bureau of Mines published a procedures guide for the fabrication of this type of instrument (Johnston and Cox 1993), and instrumented bolts were commercialized in the mid-1990's.

In 1995, researchers at the Spokane Research Center began a series of studies at five coal mines, two trona mines, and four metal/nonmetal mines to measure loading along the length of fully grouted supports. This paper reports on the roof bolt research done at one of the trona mines. The approach was to use fully grouted bolts instrumented with strain gauges to measure axial and bending loads on each bolt in the pattern, the points at which these loads developed, and how much anchorage length was available to provide support. This information can be used to select the most efficient bolt diameter, grade, length, and spacing for a given mining condition.

INSTRUMENTS

Thirty-nine bolts were instrumented with strain gauges and installed during the normal mining cycle. Twelve were 2.1 m (7 ft) long, 15 were 1.5 m (5 ft) long, 2 were 1.2 m (4 ft) long, and 10 were 0.9 m (3 ft) long. These bolts were modified by milling a slot 6 mm (1/4 in) wide and 3 mm (1/8 in) deep along the bolt and attaching five strain gauges on both sides, as shown in table 1 and figure 1. Tension tests showed that the average yield load of the bolts was 96 kN (21,500 lb) and the average ultimate load was 158 kN (35,500 lb) (figure 2). Prior to slotting, the yield load had been 106 kN (24,000 lb), and the ultimate load had been 176 kN (39,500 lb). Thus, slotting caused a 10% reduction in strength. The typical area of an unslotted bolt was approximately 2.6 cm² (0.4 in²), while that of a slotted bolt was 2.3 cm² (0.36 in²).

Table 1: Position of gauges on bolts

Bolt length, m	Distance from bolt head, cm					
	D1	D2	D3	D4	D5	L
0.9	15.3	30.5	45.6	61.0	76.3	91.4
1.2	20.3	40.6	61.0	81.3	102	122
1.5	25.4	50.8	76.2	102	127	152
2.1	35.6	71.1	107	142	178	213

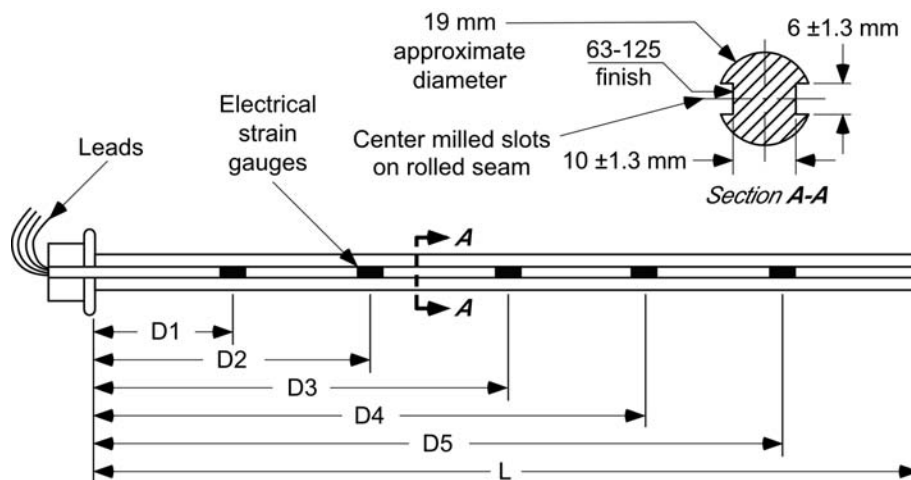


Figure 1.—Instrumented roof bolt.

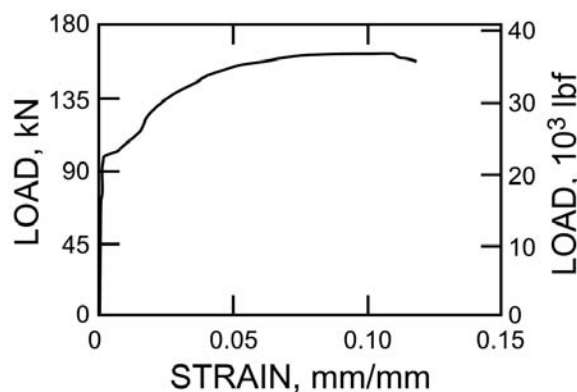


Figure 2.—Typical test of No. 6, grade 60 roof bolt.

Two types of data acquisition systems were used to measure bolt loads and roof movements. A Campbell-Scientific¹ data acquisition system, which has the capability of measuring all instruments on a continuous basis, collected readings daily on 12 of the instrumented bolts. A Omnidata Polyrecorder data acquisition system was used to read the remaining bolts immediately after installation and periodically throughout the test.

GEOLOGY

Trona is a sodium bicarbonate that forms when sodium and calcium are deposited in the presence of carbon dioxide. Sources of sodium and calcium are volcanic ash. The mineral shortite is present in the shales above and below bed 17, which is the horizon of mining interest. Shortite weakens the shale by introducing planes of fracturing.

The trona beds near Green River, Wyoming, are in the Wilkins Peak Member of the Green River Formation. These beds were depos-

ited during the Eocene about 50 million years ago as Lake Gosiute evaporated. The Green River Formation is overlain by the Bridger Formation and underlain by the Wasatch Formation. Within the Wilkins Peak Member, 25 trona beds have been identified, beginning with bed 1 (lowest) to bed 25 (highest). Bed 17 is 450 m (1,500 ft) below the surface and ranges from 2.7 to 3.0 m (9 to 10 ft) thick.

From 46 to 56 cm (18 to 22 in) of trona overlain by a green shale were found in the immediate roof. The shale contained fine-grained shortite that became coarser higher in the section. In places, the shortite was concentrated along bedding planes, which caused the shale to part easily. About 1.5 m (5 ft) above the top of the trona lay the spar trona bed, locally called the Jewell Seam, which ranged from a few centimeters to 0.3 m (1 ft) thick. This seam of trona is very pure and of a semitransparent, clear to light-brown color. This was the easiest bed to correlate in the core. Above the Jewell Seam was 0.6 to 0.9 m (2 to 3 ft) of shale very similar to the shale below the Jewell Seam, although the upper shale contained less shortite. It graded to a dark brown, finely laminated oil shale with parallel to sub-parallel bedding. Carbonaceous partings were observed along many of these bedding planes. In the floor immediately below the trona was a 0.3- to 0.6-m- (1- to 2-ft-) thick bed of oil shale like that in the roof; this oil shale graded into green shale that contained very little shortite. The amount of shortite increased with depth in each of the core holes.

In the area of test sites 1, 2, 3, and 4, 3-m- (10-ft-) long NX core holes were drilled in the roof and 1.5-m- (5-ft-) long holes were drilled in the floor. Averaged results from unconfined compressive strength tests on the core are shown in table 2.

TEST SITES

The support plan called for the 0.9-m- (3-ft-) long bolts to be installed with a Beaver drill on bore advance at 1.2-m (4-ft) spacings approximately 9 to 12 m (30 to 40 ft) behind the borer miner. After the miner was retracted, a roof bolter installed 1.5-m- (5-ft-) long bolts on 1.2- by 1.2-m (4- by 4-ft) spacings. At intersections, the 1.5-m- (5-ft-) long bolts were replaced with 2.1-m- (7-ft-) long bolts. The bolts were typically grade 60, No. 6 rebar and installed in a 25-mm (1-in) in diameter hole with a full column of fast-setting polyester resin grout. The instrumented bolts were installed in the same size hole, but used a slow-setting resin to facilitate installation.

¹Mention of specific products or manufacturers does not imply endorsement by the National Institute for Occupational Safety and Health.

Table 2: Results from tests on NX core

Material	Ultimate strength, MPa	Modulus, GPa	Poisson's ratio
Green shale	28	7.0	0.20
Oil shale . .	32	5.2	0.25
Trona	41	25	0.50

Thirteen rows of instrumented bolts were installed as part of the primary support in the panel. Four test areas were in the No. 5 entry, and two were in the No. 3 entry. A plan view of a part of the panel with test sites is shown in figure 3. At most test sites, one row of bolts was installed at mid-pillar, and one row was installed in or near the intersection. In addition, one row of bolts was installed in a pass-and-a-half entry between the No. 3 entry and the 4 room at test site 5. The trona is mined with a borer miner that creates an entry width of approximately 4.3 m (14 ft). Additional space was created in the No. 3 entry for the conveyor belt by mining another half pass, which created an entry width of 6 m (20 ft). Both types have a height of approximately 2.4 m (8 ft), and ribs are cut in a semicircle. After development mining, the panel was retreat mined by two additional cuts in each small pillar and four additional cuts in each large pillar. This additional mining was not enough to cause caving.

At test site 1, typical bolt lengths and spacings were used, while at test site 2, a bolt row with spacings of 1.5 m (5 ft) was installed along the entry. At the third test site, 1.2-m- (4-ft-) long bolts were installed in place of the 1.5-m- (5-ft-) long bolts using typical spacings. Typical bolt lengths and spacings were used again at the fourth test site. Test sites 5 and 6 were located in the No. 3 entry using typical bolt spacings and lengths.

Holes were drilled to relieve built up gas pressure in the immediate roof. These holes were 4.6 m (15 ft) deep, drilled in the center of the entry, and spaced 15.2 m (50 ft) along the length of the drivage. The gas pressure was measured at several locations with a packer placed 2.4 m (8 ft) from the roof line with a pipe connected to an air pressure gauge at the roof line. A valve was attached adjacent to the pressure gauge to allow pressure to bleed off between readings.

TYPES OF BOLT LOADING

Bolt loads can be axial, bending, and/or shear. Axial loading is generally the primary force on a steel bolt, although under some situations, high bending moments and/or shear stresses can cause bolt failure. Shear loads are impossible to estimate with this type of instrument because of the nature of the loading mechanisms and the uncertainties of load locations. However, when joint movements are present, shear loading can be critical in the design of bolt systems, and further research will be required for a better understanding of this loading mechanism.

Axial loads cause fiber stress in the bolts according to the equation

$$\sigma_a = P \div A \quad (1)$$

where σ_a = axial stress, Pa,
 P = load, N,
 and A = area of steel, cm².

A design engineer should consider several factors when calculating bending moments measured by instrumented bolts. The location of maximum bending moments may be localized and thus may not be accurately represented. Bending is measured in only one plane, but can take place in other directions, especially if high horizontal stress fields are present. (At our test sites, bolts were oriented during installation to measure the highest estimated plane of bending.) Bending moments can also be caused by joint movement, large-block rotations, and/or differential loading in mats and meshes. Bending loads cause axial fiber stress in the bolts according to the equation

$$\sigma_b = M \div S_x \quad (2)$$

where σ_b = bending stress, Pa,
 M = moment, N-m,
 and S_x = section modulus, cm³.

The total fiber stress then becomes

$$\sigma_t = \sigma_a \pm \sigma_b \leq \sigma_{max} \quad (3)$$

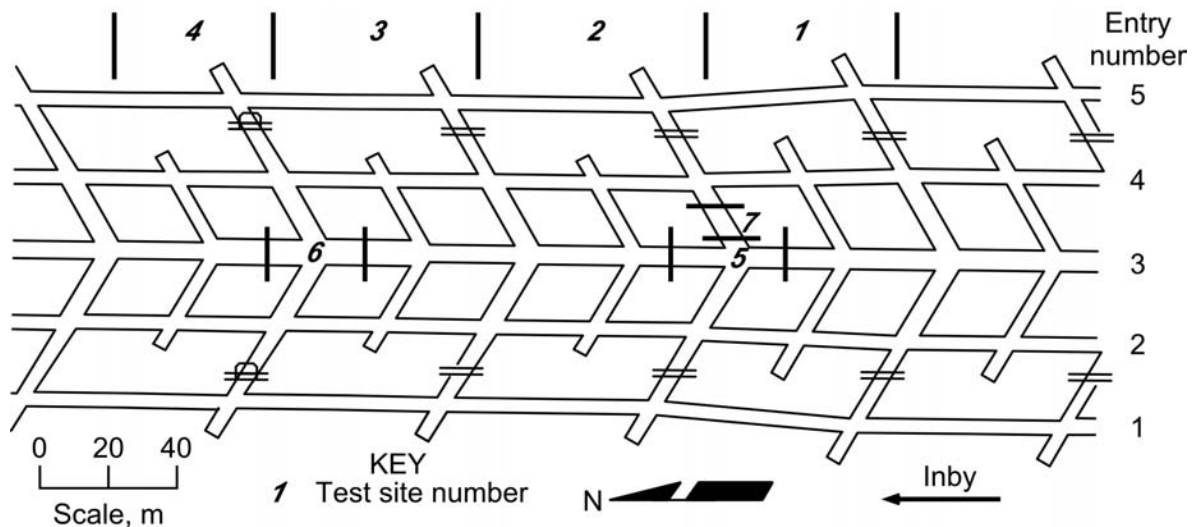


Figure 3.—Plan view of test sites.

RESULTS

where σ_t = total fiber stress
and σ_{max} = allowable fiber stress.

Total stress must be less than or equal to a design stress that has been selected on the basis of the amount of variation in geology, geometry, and in situ stress.

Another, equally important, aspect of selecting bolts for roof support is the evaluation of strain levels in the bolt (figure 2). Typical engineering design limits strain to a percentage of the yield point. Previous evaluations of strain measured on roof bolts show that, in many cases, the yield point of the steel bolt is exceeded where the roof remains stable. Fully grouted roof bolts are a stiff support system in which loads increase quickly as the bolted strata move. Rebar bolts are made from a ductile steel that can reach strain levels of 100,000 to 160,000 microstrain at ultimate load. Yielding occurs at approximately 2,000 microstrain on grade 60 rebar. Immediately after yielding, the bolt will continue to stretch with very little increase in load until the steel begins to work-harden. Thus, design strain limits should take bolt loading mechanisms—axial, bending, and/or shear—into consideration. Bolts loaded axially with little bending or shear load can reach higher strain levels than bolts subjected to high shear and bending forces.

MEASURED BOLT LOADS

Data from each instrumented bolt were evaluated in several different ways. Each bolt was calibrated in a uniaxial test machine to correlate voltage change to load change. This calibration factor was used below the steel yield point to convert voltage data to load at each of the 10 strain gauges. If a bolt section exceeded the steel's yield point, strain was calculated and load estimated from the stress-strain relationship shown in figure 2.

Axial loading was calculated by averaging the load on each side of the bolt at each gauge location. Bending moment was calculated according to equation 2. The section modulus used to calculate bending was determined both experimentally and mathematically. If a strain gauge failed, then neither axial load nor bending moment could be calculated at that bolt location. Strain was calculated directly from the voltage readings using the equation

$$\epsilon = 4\Delta V \div (GF)(ExV) \quad (4)$$

where ϵ = strain, mm/mm,
 ΔV = change, V,
 GF = gauge factor,
and ExV = excitation voltage.

Axial load, bending moments, and axial load per roof area for each instrumented bolt are shown in table 3. The bolt loads selected for this table were the maximum levels before the area was mined during the second pass. Several electrical connectors were sheared by the borer during development, and several were sheared during retreat. Those sheared during retreat showed the highest load prior to failure. Bolt loading can also be shown as a cross-sectional view of the mine entry. Figures 4 through 6 show typical axial loads on each bolt at one moment in time.

Maximum loading was observed on the instrumented bolts installed in the No. 3 entry intersections. The average of the maximum load on each of the 2.1-m- (7-ft-) long bolts was 90.6 kN (20,400 lb), and the highest load was approximately 111 kN (24,900 lb). Five out of six bolts installed in this area reached or exceeded the yield point of the steel. The average of the maximum load on each of the bolts in or near the intersections in the No. 5 entry was 45.4 kN (10,200 lb). All but two of these bolts were near the edges of the intersections. However, the two bolts in the center of the intersection showed approximately the same amount of load as those near the edge. The average of the maximum load on each of the mid-pillar bolts was 20.0 kN (4,500 lb) in the No. 3 and 34.7 kN (7,800 lb) in the No. 5 entry.

Figure 7A shows the average of maximum load of each bolt as a function of entry width, and figure 7B shows the maximum load as a function of test site. Intersection sites 5 and 6 in the No. 3 entry had the highest bolt loads. Variations in loading at intersection sites 1 through 4 in the No. 5 entry were statistically insignificant. It appears that maximum load increased from site 1 to site 4 at the mid-pillar locations. Variations from site 1 to site 3 would be expected based on changes in bolt spacing and length and grout length. However, site 1 and 4 are identical, yet show the largest difference in bolt load. This could be due to the fact that site 4 is closer to the center of the panel and would have had higher rock stresses. All maximum bolt loads were within the capacity of the bolts.

Maximum strain values were measured on the 2.1-m- (7-ft-) long bolts in the intersections in the No. 3 entry. Maximum measured strain value was 36,000 microstrain; however, several gauge locations on two bolts lost continuity, which could be due to exceeding the capacity of the strain gauge (50,000 microstrain). The loss of continuity might also indicate shearing conditions that could have led to severing of the gauge lead wires. The high microstrain readings were after second-pass mining had already passed the test site.

Stress increases caused by second-pass mining did not increase load on the bolts until the test sections were in by the borer. In some cases, load increased significantly, but in only a couple of strain gauge locations did the load approach the yield point of the steel. Bending did not appear to have a significant effect on overall bolt load. The 0.9-m- (3-ft-) long bolts appeared to have the highest maximum bending moments.

EFFECTS OF GAS PRESSURE

After installation, approximately 50% of the instrumented bolts had one or more strain gauges loaded in compression instead of tension. A typical compression loading pattern is shown in Figure 8. The magnitude of compression load change varied from 0.5 to 33 kN (100 to 7,400 lb). The average change for all of the bolts was 9 kN (2,000 lb). After 41 days, the increase in compression loading stopped and changed to tensile loading. The average time period for this transition zone was 20 days. Only 14% of the 0.9-m- (3-ft-) long bolts showed effects from gas pressure, whereas 70% of the 1.5-m- (5-ft-) long bolts and 63% of the 2.1-m- (7-ft-) long bolts were affected by gas pressure.

Table 3: Bolt load data

Length, m	Test site	Load, kN	Moment, N-m
2.1	1 intersection	49.5	112
2.1	1 intersection	65.7	5
0.9	1 mid-pillar	21.3	65
1.5	1 mid-pillar	9.8	30
1.5	1 mid-pillar	8.0	65
2.1	2 intersection	39.5	27
2.1	2 intersection	46.0	28
1.5	2 mid-pillar	29.4	43
1.5	2 mid-pillar	24.9	96
2.1	3 intersection	29.4	39
2.1	3 intersection	60.4	89
0.9	3 mid-pillar	36.0	288
1.2	3 mid-pillar	29.0	41
1.2	3 mid-pillar	40.0	85
2.1	4 intersection	19.3	22
2.1	4 intersection	51.8	40
1.5	4 mid-pillar	54.6	165
1.5	4 mid-pillar	56.2	29
0.9	4 mid-pillar	72.1	114
0.9	5 intersection	95.6	78
2.1	5 intersection	95.6	D*-35
2.1	5 intersection	95.6	118
0.9	5 mid-pillar	D	D
1.5	5 mid-pillar	D	D
1.5	5 mid-pillar	D	D
0.9	6 intersection	D	D
0.9	6 intersection	50.0	D*-353
2.1	6 intersection	95.8	97
2.1	6 intersection	110.9	14
0.9	6 mid-pillar	D	D
0.9	6 mid-pillar	16.0	253
1.5	6 mid-pillar	24.2	D*-144
1.5	6 mid-pillar	D	D
1.5	6 mid-pillar	D	D
0.9	7	49.0	145
1.5	7	31.6	35
1.5	7	53.0	D*-22
1.5	7	33.5	44
1.5	7	11.6	20

D = Electrical connector destroyed on development. D* = Electrical connector destroyed on retreat.

When instrumented bolts show compressional loading, it means that the rock surrounding the bolt is compressing as well. This is an unusual rock behavior in the immediate roof, and can be explained by gas pressure in the immediate roof. The measured gas pressure at two locations showed readings up to 0.34 MPa (50 psi). When the roof bolter was drilling gas relief holes, a noticeable amount of gas was

released, varying by location. The gas would bleed off over a considerable amount of time, causing rock pressure to subside, which in turn would cause the roof support to compress. The 0.9-m- (3-ft-) long bolts showed the least effect of this behavior, which could be because (1) they were installed closest to the face and carried more initial load and (2) they were farther from the zone of compression.

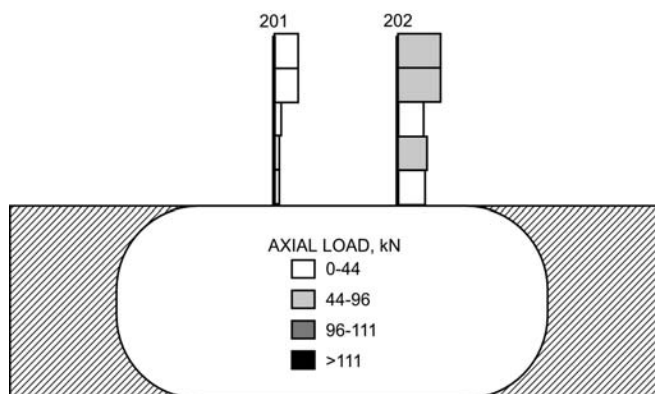


Figure 4.—Axial bolt loads at site 1 intersection.

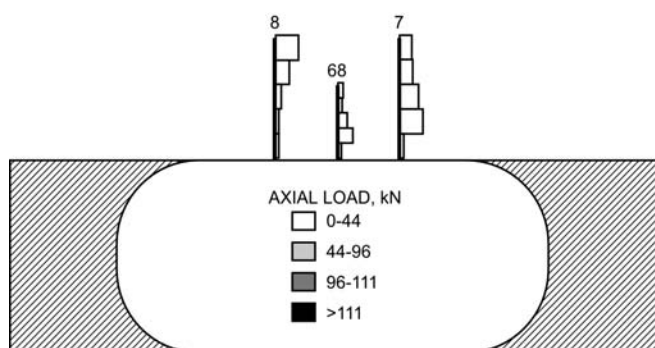


Figure 5.—Axial bolt loads at site 1 mid-pillar.

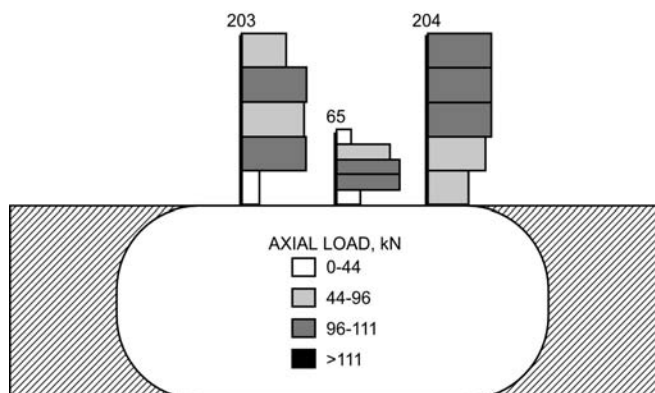


Figure 6.—Axial bolt loads at site 5 intersection.

CONCLUSIONS

The highest loads were on the 2.1-m- (7-ft-) long bolts installed in the intersections of the No. 3 entry. Average axial load on these bolts was 90.7 kN (20,400 lb), and maximum load was approximately 111 kN (24,900 lb). The ultimate strength of the grade 60, No. 6 rebar bolt used as a typical roof support was approximately 173 kN (39,000 lb). However, most of these bolts reached or exceeded the yield point of the steel. Bolt loads in the No. 5 entry intersections were significantly less than in the No. 3 entry intersections. However, many of these bolts were not positioned at the center of the intersection. Bolt

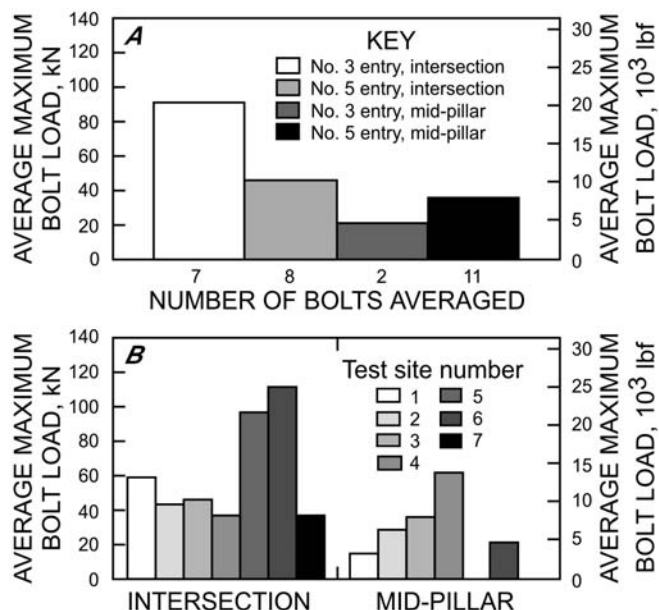


Figure 7.—Axial bolt load by (A) entry width and (B) test site.

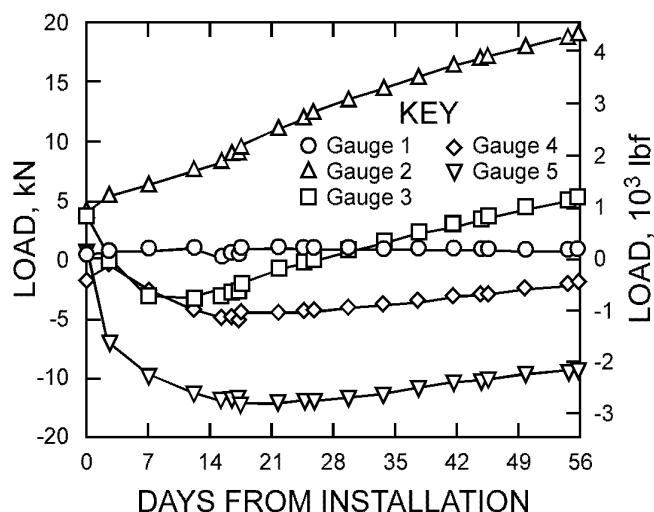


Figure 8.—Initial loading of 1.2-m-long instrumented bolt that showed compressional loads.

loading at the mid-pillar locations was approximately one-third the yield point of the steel and one-fifth the ultimate strength. Minor variations in bolt loading could be attributed to changes in bolt spacing and bolt length. Geological variations and stress changes could also have been a factor in these slight differences. Overall, readings from the instrumented bolts indicated that the roof was stable.

REFERENCES

- Dunham, R. K. Anchorage Tests on Strain-Gauged Resin-Bonded Bolts. *Tunnels and Tunneling*, vol. 8, no. 6, Sept. 1974, pp 73-76.
- Farmer I. W. Stress Distribution Along a Resin-Grouted Anchor. *Intern. J. of Rock Mechanics & Min. Sci.*, vol. 12, 1975, pp. 347-351.

Gale, W. J. Application of Field Measurement Techniques to the Design of Roof Reinforcement Systems in Underground Coal Mines. Commonwealth Scientific and Industrial Research Organization (CSRIO), Australia, 1987.

Johnston, J. L., and D. J. Cox. Instrumentation Procedures for Fully Grouted Rock Bolts. U.S. Bureau of Mines Inform. Circular 9341, 1993, 10 pp.

Larson, M., C. Stewart, M. Stevenson, M. King, and S. Signer. A Case Study of a Deformation Mechanism Around a Two-Entry Gateroad System Involving Probable Time-Dependent Deformation. Paper in *Proceedings of 14th International Conference on Ground Control in Mining*, ed. by S. S. Peng (Morgantown, WV, Aug. 1-3, 1995). Dept. of Mining Engineering, WV Univ., 1995, pp. 295-304.

Maleki, H., S. P. Signer, M. E. King, and P. A. Edminster. Evaluation of Support Performance in a Highly Stressed Mine. Paper in *Proceedings of 13th International Conference on Ground Control in Mining*, ed. by S. S. Peng (Morgantown, WV, Aug. 2-4, 1994). Dept. of Mining Engineering, WV Univ., 1994, pp. 9-17.

McHugh, Ed, and Steve Signer. Roof Bolt Response to Shear Stress: Laboratory Analysis. Paper in *Proceedings—18th International Conference on Ground Control in Mining*, ed. by S. S. Peng and C. Mark (Morgantown, WV, Aug. 3-5, 1999). Dept. of Mining Engineering, WV Univ., 1999, pp. 232-238.

Sawyer S. G., and G. J. Karabin. The Development and Use of Instrumentation for In Situ Measurement of Axial Loads in a Fully Resin-Grouted Roof Bolt. Paper in *Proceedings of 1st Symposium on Underground Mining. NCA/BCR Coal Conference & Exposition II* (Louisville, KY, Oct. 21-23, 1975). Vol. 2, 1975, pp. 90-103.

Serbousek, M. O., and S. P. Signer. Load Transfer Mechanics in Fully-Grouted Roof Bolts. Paper in *4th Conference on Ground Control in Mining*, ed. by S. S. Peng (Morgantown, WV, July 22-24, 1985). Dept. of Mining Engineering, WV Univ., 1985, pp. 32-40.

Serbousek, M. O., and Signer, S. P. Linear Load Transfer Mechanics of Fully-Grouted Bolts. Bureau of Mines Rep. of Invest. 9135, 1987, 17 pp.

Signer, S. P., and S. D. Jones. A Case Study of Grouted Roof Bolt Loading in a Two-Entry Gate Road. Paper in *9th International Conference on Ground Control in Mining: Proceedings*, ed. by S. S. Peng (Morgantown, WV, June 4-10, 1990). Dept. of Mining Engineering, WV Univ., 1990, pp. 35-41

Signer, Stephen P., and John L. Lewis. A Case Study of Bolt Performance in a Two-Entry Gateroad. Paper in *Proceedings, 17th International Conference on Ground Control in Mining*, ed. by S. S. Peng (Morgantown, WV, Aug. 4-6, 1998). Dept. of Mining Engineering, WV Univ., 1998, pp. 249-256.

Signer, S. P., C. Mark, G. Franklin, and G. Hendon. Comparisons of Active Versus Passive Bolts in a Bedded Mine Roof. Paper in *Proceedings of 12th Conference on Ground Control in Mining*, ed. by S. S. Peng (Morgantown, WV., Aug. 3-5, 1993). Dept. of Mining Engineering, WV Univ., 1993, pp. 16-23.